frontiers | Frontiers in Energy Research

TYPE Original Research
PUBLISHED 28 September 2022
DOI 10.3389/fenrg.2022.976210

OPEN ACCESS

EDITED BY
Enhua Wang,
Beijing Institute of Technology, China

REVIEWED BY
Shuang Wang,
Anhui University of Science and Technology, China
Nikolay Kiktev,
National University of Life and Environmental Sciences of Ukraine, Ukraine

*CORRESPONDENCE
Liguo Han,
hlg2109@163.com

SPECIALTY SECTION
This article was submitted to Process and Energy Systems Engineering, a section of the journal Frontiers in Energy Research

RECEIVED 27 June 2022
ACCEPTED 25 August 2022
PUBLISHED 28 September 2022

CITATION
Zhao L, Han L, Zhang H, Ge M, Yang S and Jin X (2022), Influence of particle characteristics on dynamic characteristics of tail beam under coal rock caving impact.
Front. Energy Res. 10:976210.
doi: 10.3389/fenrg.2022.976210

Influence of particle characteristics on dynamic characteristics of tail beam under coal rock caving impact

Lijuan Zhao[1,2], Liguo Han[1]*, Haining Zhang[1], Man Ge[3], Shijie Yang[1] and Xin Jin[1]

[1]School of Mechanical Engineering, Liaoning Technical University, Fuxin, China, [2]The State Key Lab of Mining Machinery Engineering of Coal Industry, Liaoning Technical University, Fuxin, China, [3]Quality Center, Shandong Yankuang Intelligent Manufacturing Co., Ltd, Jining, China

In order to improve the accuracy of simulation parameters used in the discrete element simulation test of a fully mechanized top-coal caving process and further explore the intelligent fully mechanized coal caving technology, this research work studies the influence of particle characteristics on the dynamic response of tail beams under the impact of caving coal rock in the process of coal caving. Based on the interface technology, the EDEM–RecurDyn–AMESim multi-domain collaborative simulation top-coal caving support is a built-model of a hydraulic mechanical integration system for scraper conveyors, which is used to simulate the coal caving process of the top-coal caving support to obtain the vibration signal of the tail beam of the top-coal caving support. This model can also be used to convert it into a two-dimensional time-spectrum image using the short-time Fourier transform (STFT) algorithm. Several groups of simulation tests were carried out on different particle radii, standard deviation of particle normal distribution, and particle slenderness ratio. The time-domain information and frequency-domain information obtained from the simulation were analyzed and compared. Combined with the vibration signal of the tail beam measured on the spot, the optimal setting parameters of the multi-field collaborative virtual prototype simulation were obtained. Compared with the data measured in the coal mine, the relative error of the maximum vibration value of the tail beam is only 3.8%, the minimum relative error is 5.5%, and the relative error of the root mean square value is 14%, which verifies the method and simulation results. This method solves the problems of difficult on-site sampling, high risk coefficient, and high test cost and promotes the development of an intelligent process of coal mining.

KEYWORDS

top-coal caving, tail beam, EDEM parameter calibration, multi-domain collaborative simulation, STFT

1 Introduction

Fully mechanized top-coal caving has become the main method of thick seam mining in China. Intelligent coal mining is the only way for high-quality development of the coal industry (Wang et al., 2022). Coal gangue identification is the key core technology of fully mechanized top-coal caving, which has an important influence on the coal recovery rate and quality of recovered coal. By studying the vibration signal analysis method and feature extraction algorithm of coal gangue impact tail beams, a vibration signal identification method based on the coal gangue impact tail beam is constructed to determine the switching time of the tail beam. Based on the virtual prototype technology, the method of using discrete element software to simulate the ground pressure, movement law of top-coal fully mechanized caving, and caveability has been adopted by a large number of scholars. Yu et al. (2021) used the discrete element numerical simulation method to study the evolution mechanism of the overburden rock layer in the process of surface movement and deformation under the condition of large mining depth and provided theoretical reference for the law of surface movement and deformation under the condition of large mining depth fully mechanized caving mining. Zhang et al. (2016) studied the formation mechanism of overburden separation in fully mechanized top-coal caving mining, simulated the dynamic development process and distribution law of separation in working face with discrete element software, and determined the development position of maximum separation. Mao et al. (2019) took ZF15000/28/52 export topping coal release hydraulic support as the research object and used EDEM discrete element simulation software to establish a three-dimensional simulation model to study the coal release process and the breaking law between the direct top and basic top, which provided a new idea for studying the coal release process. Liu et al. (2018) used the discrete element method of continuum mechanics to establish a numerical simulation model of hydraulic support to study the ratio of initial support force to rated working resistance, which provides a reference for the selection of working resistance of hydraulic support for large mining height support (Yang and Zeng (2021, 2022). In order to improve the coal gangue classification and recognition effect, a coal gangue classification and recognition method of "multi-information fusion" based on the "parallel voting system (PVS)" was proposed. Wang et al. (2013) used discrete element software to establish a three-dimensional numerical simulation model of fully mechanized top-coal caving release to study the top-coal release pattern, which is important for improving the coal mining rate. Zhao et al. (2020a) studied the effect of particle radius on roller load characteristics and coal fall during the simulation of the spiral drum cutting process by discrete element software, and the simulation results were closer to the theoretical values by using particles with a radius of 12 mm to build the coal wall, which provided a reference for the selection of particle radius in the simulation of coal mining machine cutting process using EDEM discrete element simulation software and laid the foundation for the study of the reliability of mining equipment (Zhao et al., 2020b), identification of coal gangue in the fully mechanized coal (Zhang et al., 2021), and adaptive height control of coal mining machine (Wang et al., 2021). Particle characteristics have an important influence on the accuracy of discrete element simulation tests and have been studied accordingly in the fields of medicine (Bharadwaj et al., 2010), agriculture (Liu et al., 2021; Zhang et al., 2022), and geotechnical engineering (Xinliang et al., 2021). Researchers at home and abroad use discrete element simulation software to study the key technologies and equipment of fully mechanized top-coal caving, but there is a lack of relevant research on the particle characteristics that affect the simulation results. In fact, due to the bad working conditions and complex environment, the occurrence conditions of the top coal, the coal discharge mode of the tail beam, the kinematic parameters of the scraper conveyor, the gradient characteristics of the hydraulic system, and the interaction between the roof beam and the roof will directly or indirectly affect the top-coal caving process of the top-coal caving support that exists underground. The way to obtain the dynamic characteristics of the tail beam through industrial tests is restricted by the underground environment, and safety factors such as explosion-proof need to be considered. The test cost is high, and the implementation is difficult. Therefore, how to quickly and accurately measure the dynamic characteristics of the tail beam of the top-coal caving support is a difficult problem in the implementation of intelligent mines such as coal gangue identification.

Based on the virtual prototype technology, in this study, a multi-domain collaborative simulation model of top-coal caving support using Creo, RecurDyn, AMESim, and EDEM is built; a simulation model of top-coal caving support and scraper conveyor using Creo and RecurDyn is established; and a discrete element top-coal model using EDEM is established. Based on the DEM–MBD interface, the mechanical system model of the EDEM–RecurDyn bi-directional coupling coal drawing mechanism is built, and the hydraulic system model of the support is established based on AMESim. The EDEM–RecurDyn–AMESim multi-domain collaborative simulation model of the top-coal caving support coal caving machine liquid integrated system based on the interface technology has the advantages of more real simulation of the top-coal caving process, high accuracy, and convenient collection of the data. This system model is used to study the dynamic response of the tail beam of the top-coal caving support. By analyzing the influence of particle characteristics on the dynamic characteristics of the tail beam of the top-coal caving support during the simulation of EDEM discrete element software, different particle radii, particle distribution, and particle shape are selected for modeling and simulation, and reasonable simulation parameters are determined. The mind map of the research process is shown in Figure 1, and the process has good theoretical significance and engineering application value for improving the accuracy of the test results.

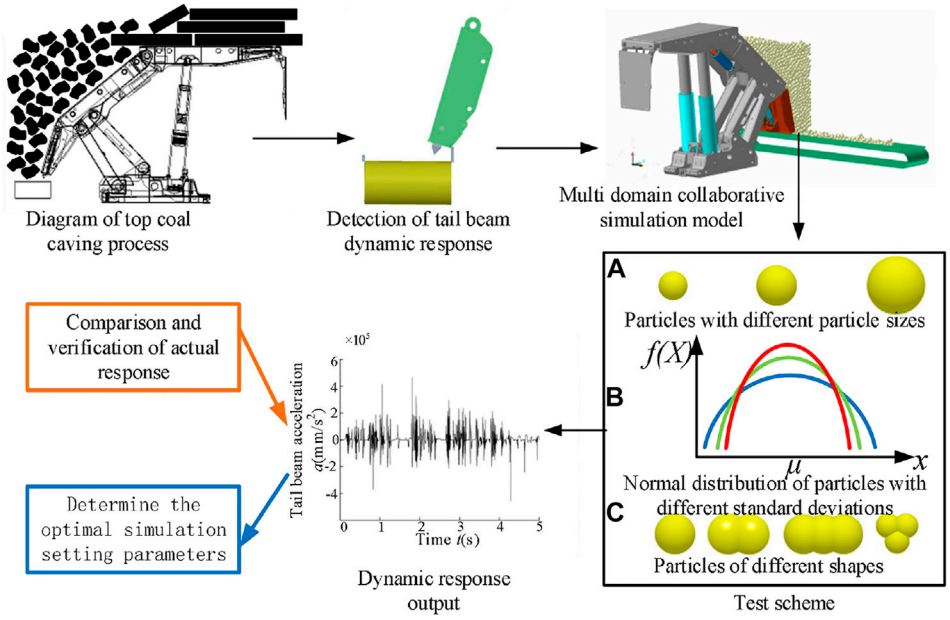

FIGURE 1
Research process mind map.

2 Engineering background

The 1109 fully mechanized top-coal caving face of Baiyinhua No. 4 mine is located in the southeast of the first mining area, with a mining trend of 668 m, a tendency length of 230 m, and an inclination of 8–12°. The coal seam is 39–44 m in full thickness here, with 3–5 layers of gangue; the single layer of gangue is 0.35 m–1.9 m in thickness; and the accumulated thickness is 4.2 m–5.0 m, which is developed in layers within the working face. The top plate of the coal seam is dark gray and gray mudstone, and the bottom plate of the coal seam is gray-white muddy cemented fine sandstone. According to the thickness of the coal seam and its conditions, the integrated mechanized coal release toward the long wall mining method is adopted. The empty area is treated using the fully caving method. The coal mining machine has a mining height of 3.5 m and a cutting depth of 0.6 m and uses the back mining process. The average thickness of the coal caving is 10.5 m, the coal caving adopts one mining and one releasing, and the coal caving step is 0.6 m. The coal caving lags behind the coal mining machine by 15 m and adopts a multi-round, equal amount, and sequential coal caving process. Coal caving is carried out from the top to bottom and adopts two rounds to release the full height. First, the metal net at the insert of the released support is cut off, the coal opening is opened, the quantity of coal of about 3 m is released, and the coal opening is closed. Then, it proceeds to the next one until the end of the first round. Then, the second round of coal caving is carried out, which is also in accordance with the sequence of the first round of coal caving; from the top to bottom, the coal caving port is opened until gangue occurs, the coal caving port is closed, and then the next coal caving is carried out until the end of the second round.

3 Multi-domain modeling way of comprehensive top-coal caving system

The release of coal from caving supports is a complex dynamic process, and the advantages of simulation software in different fields should be fully utilized to build a collaborative simulation model with high reliability and an easy interface to transfer information.

3.1 Three-dimensional solid model construction

According to the relationship between the grade of the top plate and frame type and support strength of the 1109 comprehensive caving working face of Baiyinhua mine, ZFY12000/25/42D type coal caving support and SGZ1000/1400 type rear scraper conveyor are used as engineering objects, and their main technical parameters are shown in Tables 1 and 2. ZFY12000/25/42D type support is a two-column cover type, with an insert plate type coal caving mechanism. The tail beam with a telescopic insert plate is installed at the lower end of the cover beam, supported by a tail beam jack. It can swing at a certain range for loosening the top coal. When the coal release

TABLE 1 Main technical parameters of ZFY12000/25/42D type support.

Project	Parameter	Project	Parameter
Center distance (mm)	1750	Initial support force (kN)	7916
Working resistance (kN)	12000	Maximum height (mm)	4200
Minimum height (mm)	2500	Base width (mm)	1530
Average support strength (MPa)	1.24-1.31	Average specific pressure of bottom plate (MPa)	2.48

TABLE 2 Technical parameters of SGZ1000/1400 scraper conveyor.

Project	Parameter	Project	Parameter
Conveying capacity (T/h)	2200	Installed power (kW)	2 × 700
Scraper chain form	Medium double chain	Scraper chain speed (mm/s)	1300
Scraper chain specification (mm)	Φ42*146	Specification of middle trough (mm)	1500 × 1000 × 345

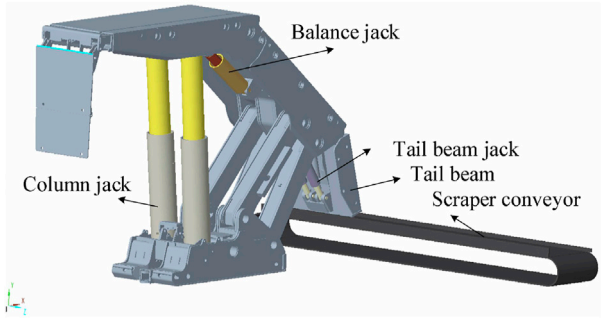

FIGURE 2
Three-dimensional solid model.

mechanism is closed, the insert plate extends to block the gangue from flowing into the rear conveyor. When the coal release mechanism opens, the insert plate is retracted to prevent it from colliding with the rear conveyor. Based on Creo 8.0, three-dimensional solid models of components are built and assembled, and the final assembly solid model is shown in Figure 2.

3.2 Model construction of caving support machine liquid system

The 3D model created by Creo8.0 is checked for interference, and then the assembly of caving supports and scraper conveyor is imported into RecurDyn in the x_t format, and the material and quality of each part are defined while the constraints between the parts are added according to the actual working principle of top-coal caving, and finally, the dynamics simulation model of top-coal caving support–scraper conveyor in the RecurDyn environment is established, as shown in Figures 2, 3.

As shown in Figure 4, the hydraulic system model of the top-coal caving support is established based on the AMESim environment (Wu, 2010). In Figure 4, the red dotted line is connected to the RecurDyn–AMESim simulator interface module. The displacements x_i of the column, tail beam jack, and balancing jack are the five outputs of the AMESim model, which are input into RecurDyn by AMESim. The force Fi of the column, tail beam jack, and balance jack are input into the piston of the hydraulic cylinder in AMESim by RecurDyn to realize the linkage of the hydraulic cylinder.

3.3 Bi-directional coupling model construction of virtual prototype of top-coal caving support

Top coal is broken, and caving is the result of multi-factor coupling. Geometric parameters of coal caving mechanism, movement mode of pillars and tail beams, occurrence conditions of coal rock, and interaction between tail beams and coal rock will directly or indirectly affect the process of top-coal caving and its dynamic characteristics. Based on the interface of EDEM and RecurDyn, the two-way coupling model of a virtual prototype of top-coal caving support is constructed by adopting the discrete element method–multi-body dynamics (DEM-MBD) two-way coupling mechanism. The coupling calculation principle is shown in Figure 5.

Within the unit time step, RecurDyn transmits the motion information of the components to the corresponding coupling component Walls of EDEM, which will contact and collide with particles in EDEM according to the motion information.

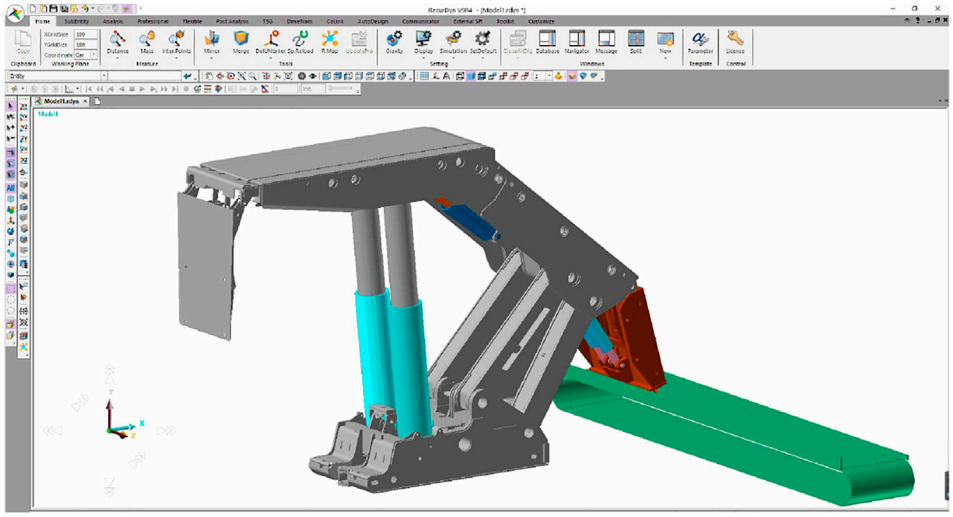

FIGURE 3
Dynamic simulation model of top coal caving support–scraper conveyor.

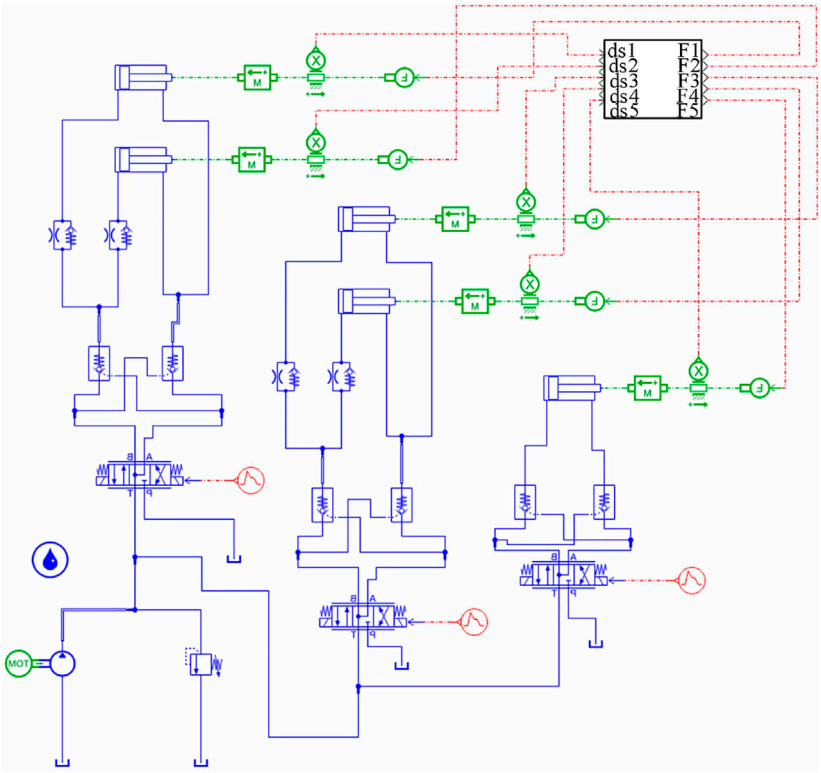

FIGURE 4
AMESim model.

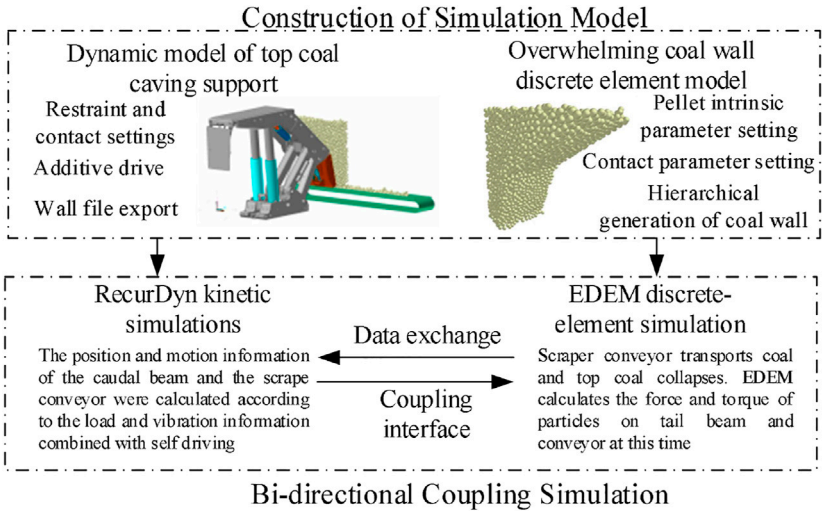

FIGURE 5
EDEM–RecurDyn coupling calculation principle.

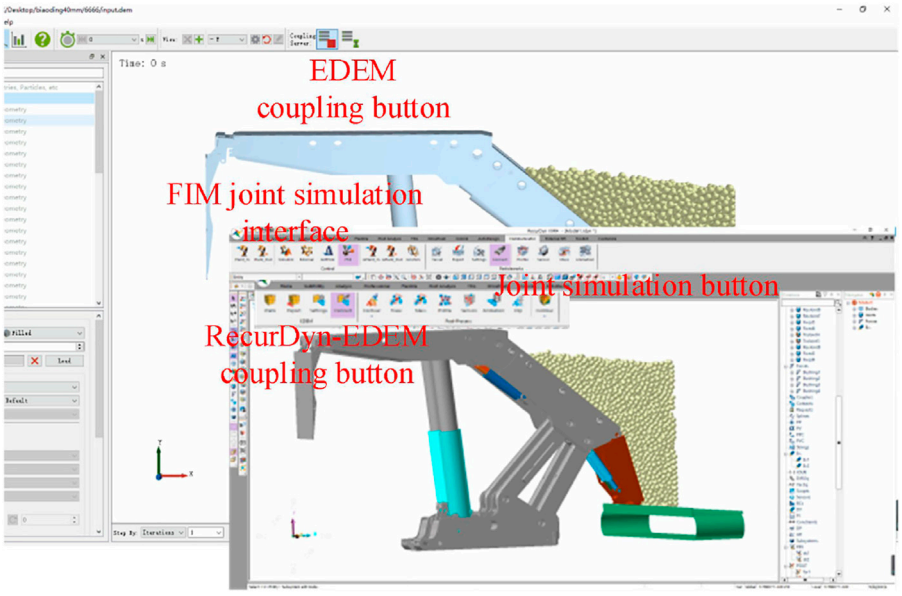

FIGURE 6
RecurDyn–EDEM bi-directional coupling simulation interface.

The movement of the part position causes the size and direction of the force on the particle body to change, at which time EDEM calculates the force and moment of the particle acting on the coupling part and returns them to RecurDyn. At this time, a simulation of the unit time step is completed. In the next step, the component in RecurDyn will calculate the new displacement and speed of the component based on the new force and torque and its own driving information and complete the data exchange of each wheel in a cycle. This cycle continues until the end of the coupling simulation. The RecurDyn–EDEM coupling simulation interface is shown in Figure 6. Taking the status of top-coal caving with support as the research object, the simulation state of top-coal caving is shown in Figure 7. The

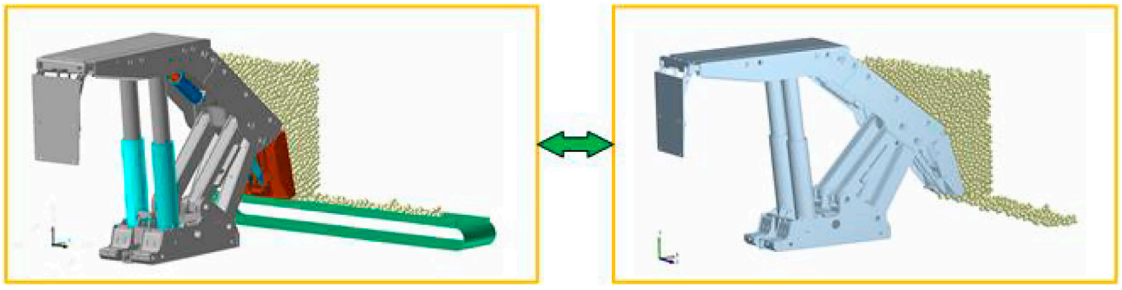

FIGURE 7
RecurDyn–EDEM bi-directional coupling simulation state.

multi-domain collaborative simulation method based on a virtual prototype interface technology is shown in Figure 8.

4 The research project

Discrete element analysis is one of the important tools to study rock mechanical behavior and improve the basic theory of rock mechanics (Chen et al., 2021). The main research content of this study is the influence of coal rock particle characteristics on the dynamic characteristics of the tail beam. Considering the influence of particle size, distribution, and shape of coal rock particles on vibration characteristics of the tail beam, three research schemes are designed as follows:

4.1 Model design for different particle sizes of coal and rock

Simulations using discrete particles of different radii can have some influence on the experimental results (Zhao et al., 2020a). Excessive particle size affects simulation accuracy, and simulation tests with small particle size take a long time. Three caving coal rocks with uniform diameter distribution (20 mm, 40 mm (Wang et al., 2015), and 60 mm) were used to simulate the coal caving process, and the optimum particle size corresponding to the actual conditions was obtained.

4.2 Model design for different coal rock particle distributions

Particle morphology and gradation are important factors affecting the movement of debris particle flow (Cui et al., 2021). The particle size distribution of crushed and collapsed debris of top coal is different under actual conditions. To explore the influence of particle distribution on simulation tests, normal particle size distribution should be chosen in EDEM (Luo et al., 2016; Han et al., 2021). Three particle models with 1 expectation and 0, 0.05 (Wang et al., 2019), and 0.1 standard deviations are used to simulate the top-coal caving process, as shown in Figure 9.

4.3 Model design for different particle shapes of coal rock

The irregular shape of particles can significantly affect the collapse motion characteristics of particle columns (Zhang et al., 2019). Because there are a lot of caving coal rocks with different shapes in the process of top-coal caving, the traditional circular particle simulation may not accurately reflect the effect of the shape of coal rock particles. Therefore, the slenderness ratio (Bian et al., 2015) defined by formula (1) is selected as the parameter to describe the particle shape, and four groups of coal rock particles with slenderness ratios of 1, 1.5, 2, and N/A (Hu and Chen, 2019) are generated to explore the influence of particle shape on the simulation of the top-coal caving process. The particle size and shape are shown in Figure 10.

$$A = \frac{L}{D}, \tag{1}$$

where L is the total length of the particle and D is the diameter.

5 Influence of coal rock particle characteristics on dynamic characteristics of coal caving

Taking RecurDyn as the main control platform for multi-domain collaborative simulation, the three modules are integrated based on AMESim, RecurDyn, and EDEM indirect interface modules. According to the sampling theorem (Xi, 2020), the sampling frequency is determined as fs = 2000Hz, and the simulation time is 5S by Eqs. 2–4. In the simulation test of top-coal caving, friction and violent vibration occur between the tail beam and collapsed coal rock. A sensor is set in the abdomen of the

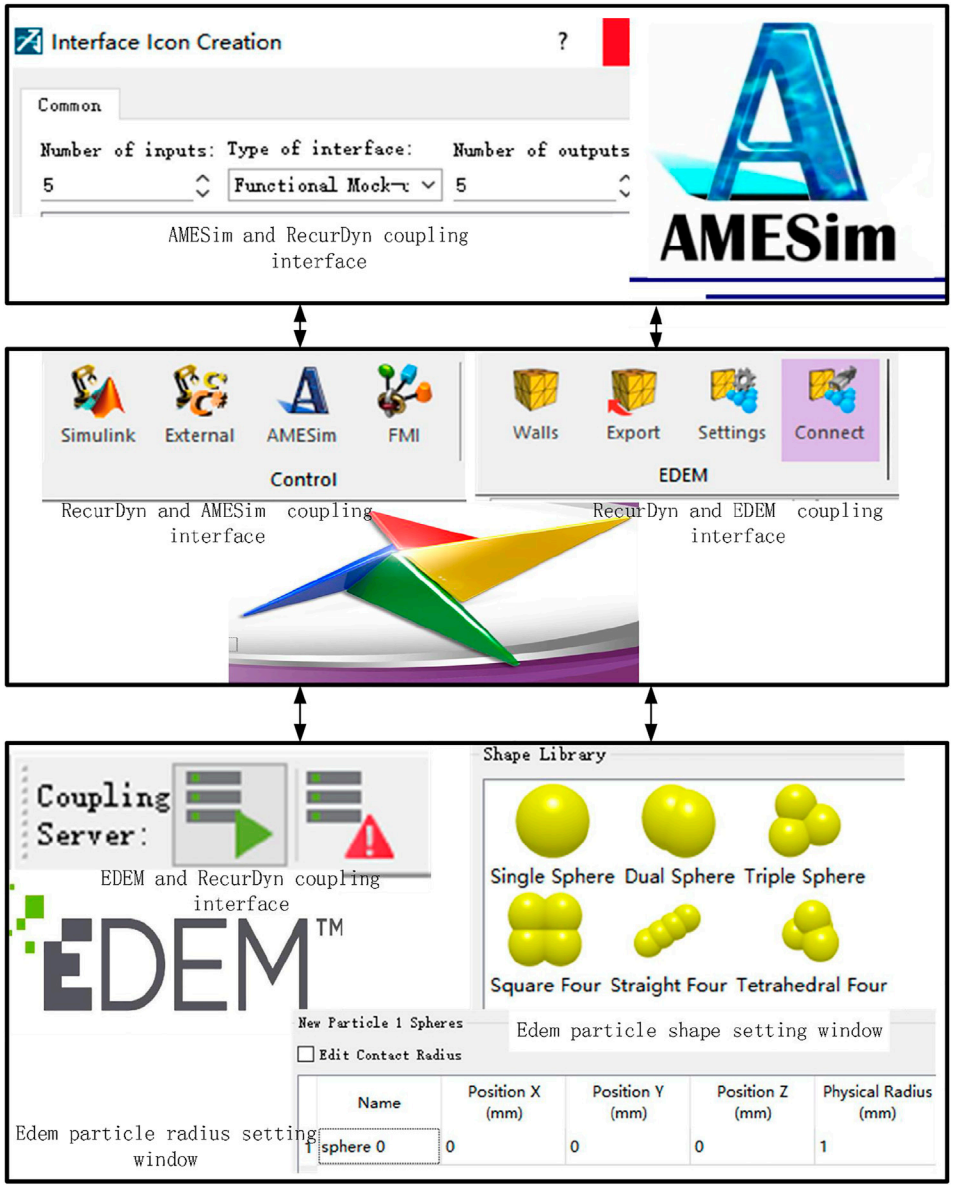

FIGURE 8
Multi-domain collaborative simulation method.

tail beam. After the simulation, data are extracted to identify the dynamic characteristics of the coal caving process.

$$f_s = \frac{1}{\Delta t}, \tag{2}$$

$$f_n = \frac{1}{2\Delta t} = \frac{f_s}{2}, \tag{3}$$

$$\Delta t < \frac{1}{2f_{\max}}, \tag{4}$$

where f_s, f_n, and $f_{\max}$ are the sampling frequency, Nyquist frequency, and highest frequency of the signal.

5.1 Influence of particle size on dynamic characteristics of coal caving

The three-dimensional solid model from Figure 1 shows that the tail beam rotates around the Z-axis, and the vibration in the fixed z-direction is negligible. According to the three models with different particle radii of top coal in Scheme 1, time-domain diagrams of tail beam vibration acceleration corresponding to different particle radii are shown in Figures 11, 12, and 13.

From Figures 11, 12, and 13, it can be seen that the tail beam is impacted by the non-linear alternating load during

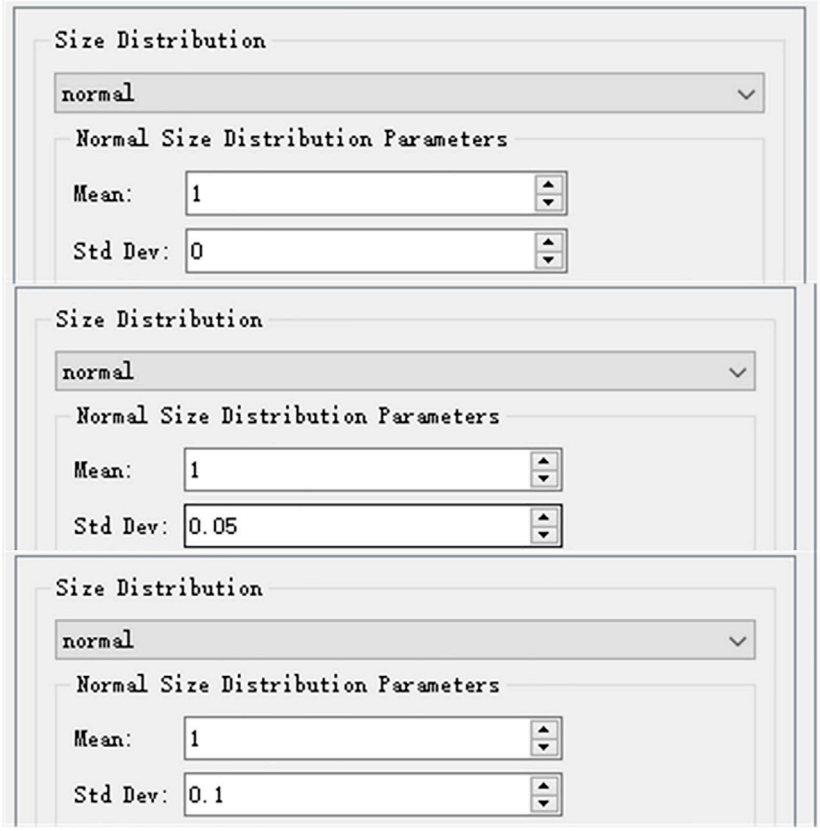

FIGURE 9
EDEM particle distribution settings.

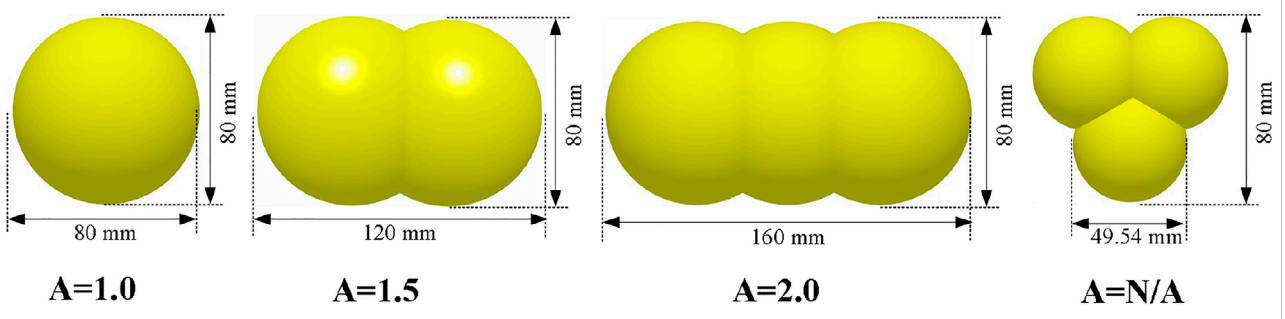

FIGURE 10
Particle shape.

coal caving, resulting in violent vibration, and the intensity of vibration in the X-direction is much greater than that in the Y-direction. Therefore, the acceleration of the most intense directional vibration is selected as the representative of the dynamic response of the tail beam, and the X-direction acceleration value of the tail beam is obtained, as shown in Table 3. As can be seen from Figures 11, 12, and 13, with the increase in particle radius, the frequency of data fluctuation decreases gradually because with the increase in particle radius, the number of collisions between particles decreases, and the impact kinetic energy on the tail beam decreases. When the particle size is different, not only the

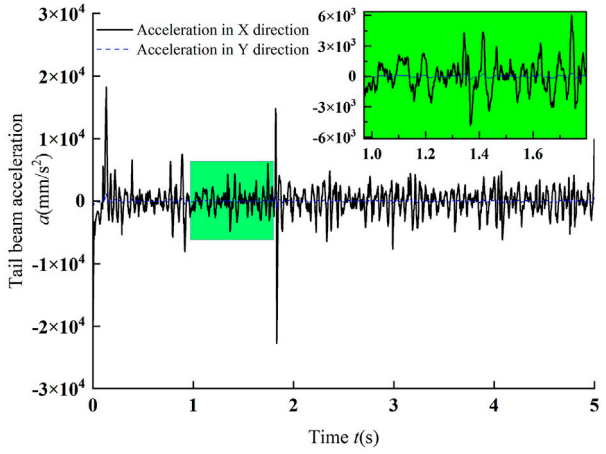

FIGURE 11
Time-domain diagram of tail beam vibration with 20 mm particle size.

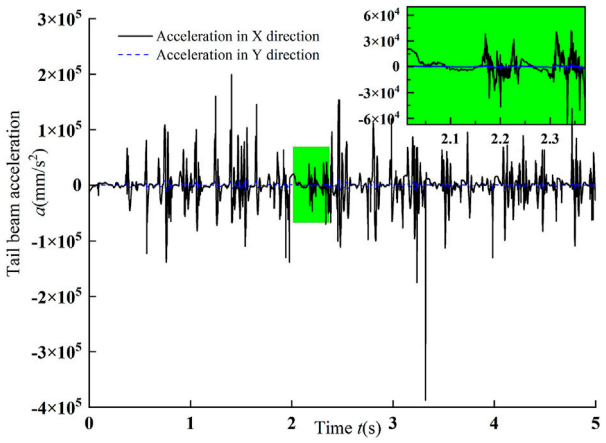

FIGURE 12
Time-domain diagram of tail beam vibration with 40 mm particle size.

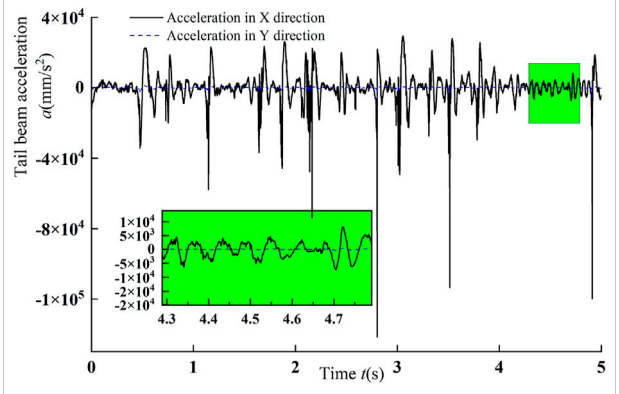

FIGURE 13
Time-domain diagram of tail beam vibration with 60 mm particle size.

vibration amplitude but also the vibration frequency is variable. The change in frequency cannot be identified by time-domain analysis alone. Therefore, the STFT algorithm (Cai et al., 2020) was used to convert the time-domain signal of the tail beam acceleration for different particle size working conditions into a time–frequency spectrum image, as shown in Figure 14.

From Table 3, it can be seen that the vibration amplitude increases first and then decreases with the increase in particle radius. When the particle radius is 20 mm, the vibration signal is symmetrical, and the absolute maximum and minimum values are not significantly different. Figure 14A shows that the main frequency energy is mainly distributed at 20 Hz under operating conditions; Figure 14B shows that the main frequency energy is mainly distributed at 25 Hz under operating conditions. Figure 14C shows that the main frequency energy is mainly distributed at 12 Hz under operating conditions. It can be seen from Figure 12 that the energy distribution frequency of the signal main frequency increases first and then decreases with the increase in particle radius. This is mainly due to the remarkable difference in amplitude, frequency, period, and other characteristics of vibration signals obtained by the tail beam under different particle radius coal caving conditions.

5.2 Influence of particle distribution on dynamic characteristics of coal caving

Based on the three models with different top-coal particle distributions in Scheme 2, Figure 15 shows the time-domain diagrams of tail beam vibration acceleration corresponding to different particle distributions, and the vibration acceleration values of the tail beam are calculated as shown in Table 4. Figure 16 shows the time–frequency spectra of tail beam vibration acceleration corresponding to different particle distributions.

It can be seen from Figure 15 that the amplitude of vibration increases first and then decreases with the increase in standard deviation. It can be seen from Table 4 and Figure 15 that when the standard deviation is not 0, the vibration signal is more symmetrical, and there is little difference between the absolute maximum value and minimum value. As can be seen from Figure 16A, when the standard deviation is 0, the dominant frequency energy is mainly distributed at 25 Hz. It can be seen from Figure 16B

TABLE 3 Acceleration values at different particle sizes.

Acceleration (mm/s^2)	Particle size 20 mm	Particle size 40 mm	Particle size 60 mm
Effective value	2316.19	26,869.83	8632.28
Maximum	18,233.17	199,548.98	29,432.41
Minimum	−22828.49	−387501.37	−141676.83

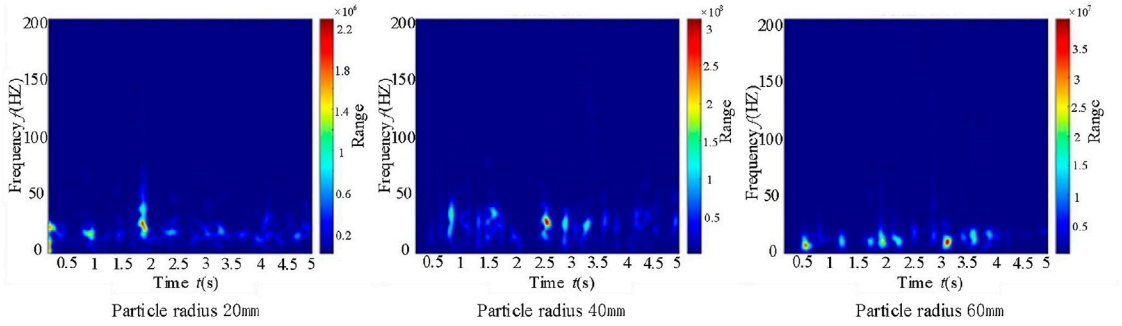

FIGURE 14
Time–frequency spectra of tail beam vibration with different particle sizes.

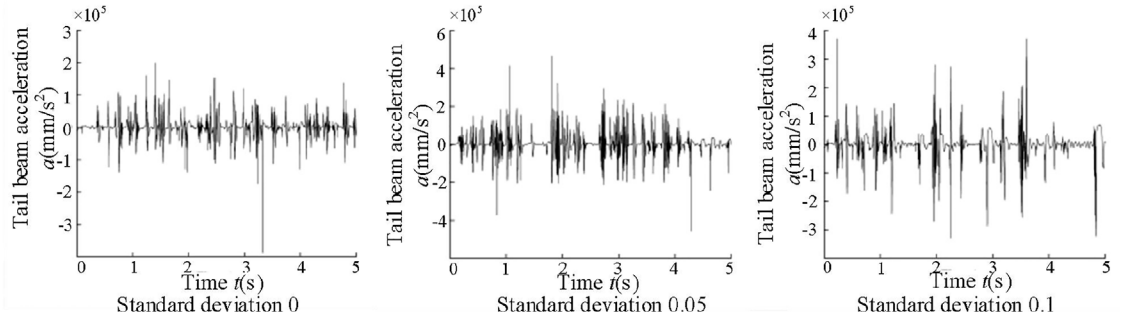

FIGURE 15
Time-domain diagram of tail beam vibration under different particle distributions.

TABLE 4 Acceleration values under different particle distributions.

Acceleration (mm/s^2)	Standard deviation 0	Standard deviation 0.05	Standard deviation 0.1
Effective value	26,869.83	52,247.68	44,990.25
Maximum	199,548.98	464,818.02	372,169.69
Minimum	−387501.37	−457009.50	−328612.36

that the main frequency energy is mainly distributed at 35 Hz with a standard deviation of 0.05. It can be seen from Figure 16C that the main frequency energy is mainly distributed at 50 Hz and 15 Hz when the standard deviation is 0.1. As can be seen from Figure 16, the frequency of the main frequency energy distribution of the

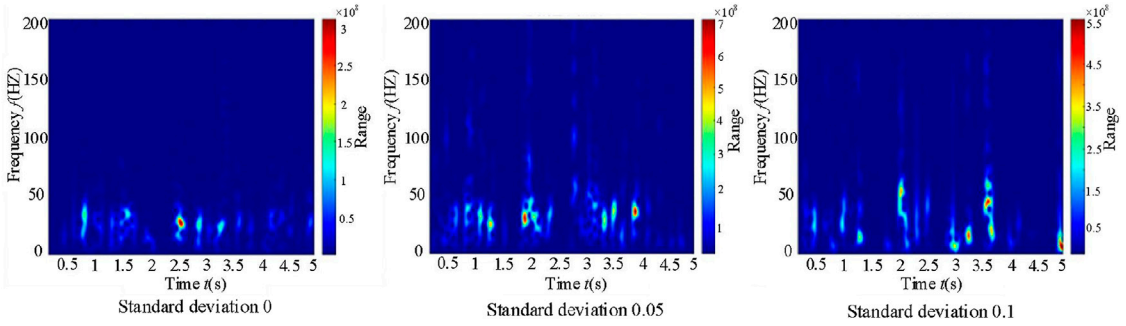

FIGURE 16
Time–frequency spectra of tail beam vibration with different particle distributions.

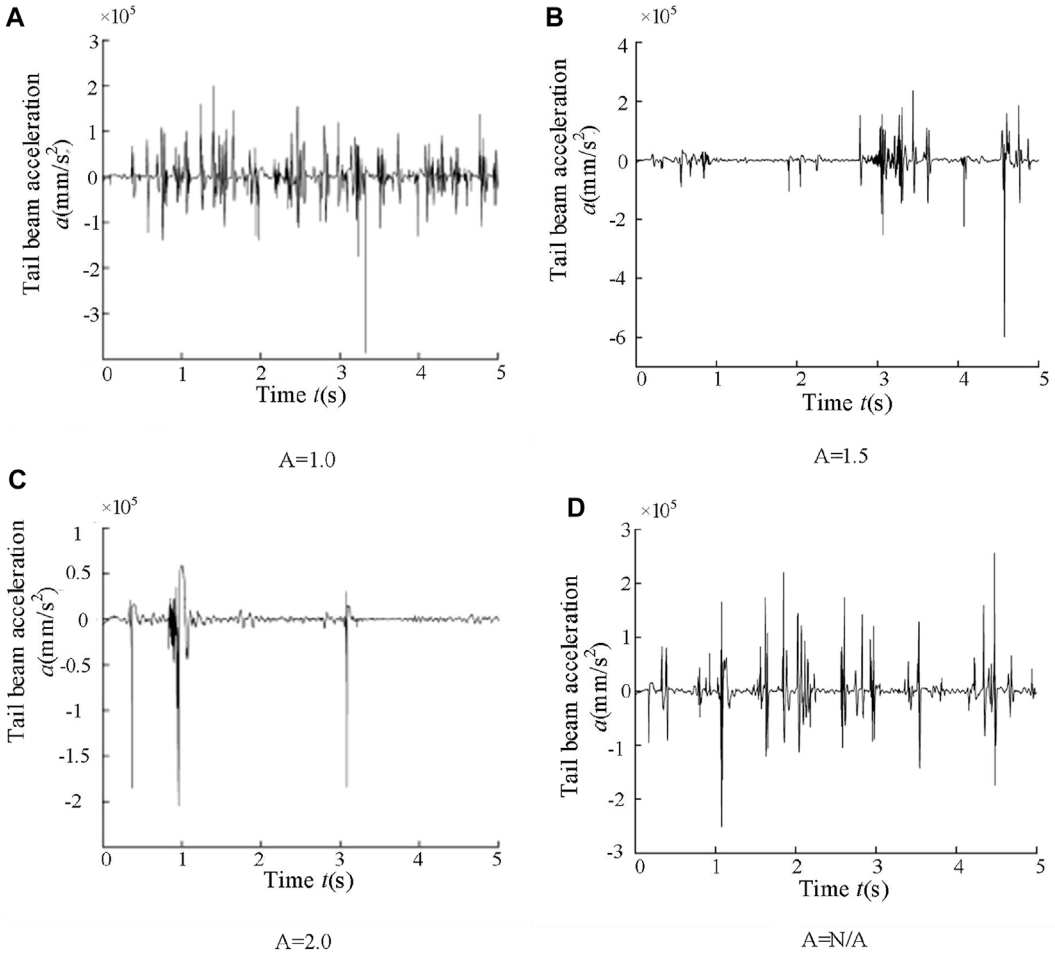

FIGURE 17
Time–domain diagram of tail beam vibration under different particle shapes.

signal increases with the increase in the standard deviation. The standard deviation reflects the degree of dispersion of particles. With the increase in standard deviation, the discrete degree of the particle radius increases. From the analysis results, it can be concluded that setting a certain value of standard deviation is of great significance for high-accuracy

TABLE 5 Acceleration values under different particle shapes.

Acceleration (mm/s^2)	A = 1.0	A = 1.5	A = 2.0	A = N/A
Effective value	26,869.83	28,233.66	11,323.35	23,376.82
Maximum	199,548.98	235,731.35	59,230.08	256,065.99
Minimum	−387501.37	−598639.58	−204739.81	−251748.02

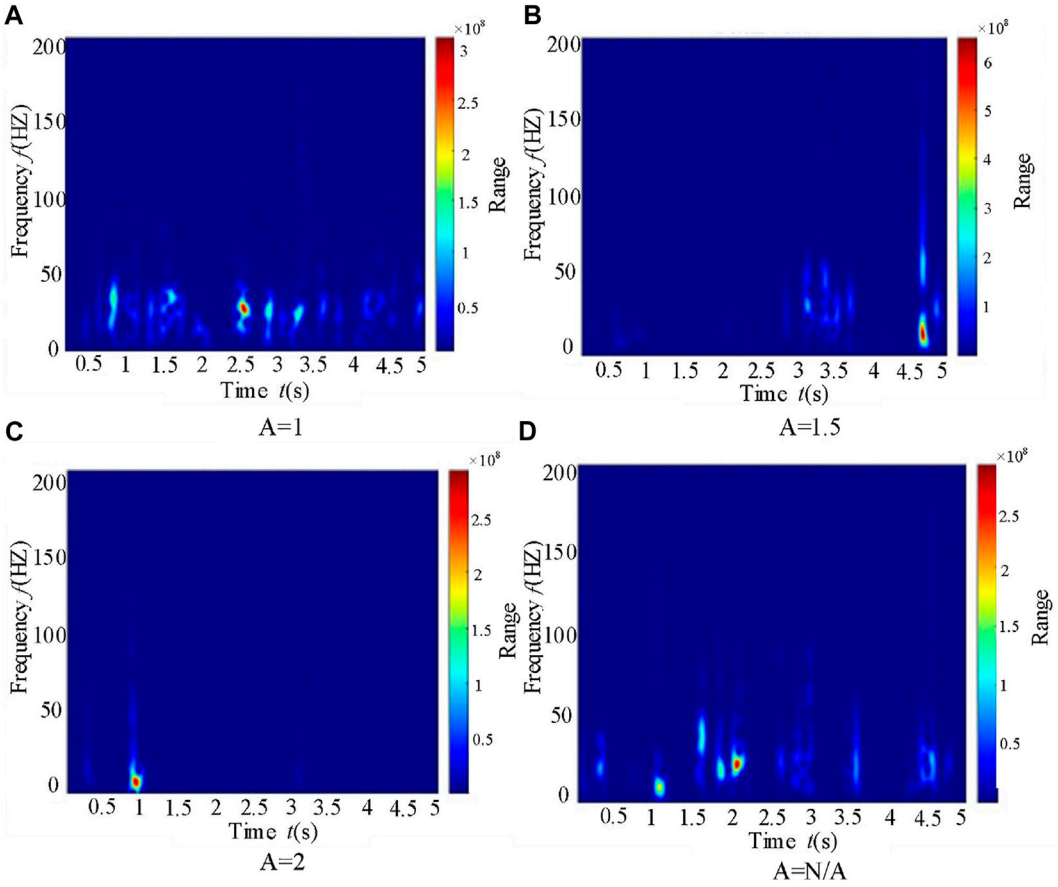

FIGURE 18
Time–frequency spectra of tail beam vibration with different particle shapes.

simulation of the coal process at the top of the hydraulic support.

5.3 Influence of particle shape on dynamic characteristics of coal caving

For the four models with different top-coal particle shapes in Scheme 3, Figure 17 shows the time-domain diagrams of tail beam vibration acceleration corresponding to different particle shapes, and the vibration acceleration values of the tail beam are calculated as shown in Table 5. Figure 18 shows the time–frequency diagram of tail beam vibration acceleration corresponding to different particle shapes. It can be seen from Figure 17 that the fluctuation time of the vibration signal gradually decreases with the increase in the slenderness ratio (from 1 to 2), and the amplitude first increases and then decreases with the increase in the slenderness ratio. From Table 5 and Figure 17, it can be seen that the vibration signal is the most symmetrical when

the slenderness ratio is A = N/A, and the maximum and minimum values are basically the same. It can be seen from Figure 18A that the main frequency energy is mainly distributed at 25 Hz when A = 1. It can be seen from Figure 18B that the main frequency energy is mainly distributed at 15 Hz when A = 1.5. It can be seen from Figure 18C that the main frequency energy is mainly distributed at 10 Hz when A = 2.0. It can be seen from Figure 18D that the main frequency energy is mainly distributed at 23 Hz when A = N/A. It can be seen from Figure 17 that the frequency of energy distribution of the main frequency of the signal decreases gradually with the increase in the slenderness ratio (from 1 to 2). The energy distribution of the main frequency at A = N/A is similar to that at A = 1. Different particle shapes represent the shape of the smallest unit composed of coal and rock mass. Through the aforementioned analysis, it can be seen that particle shape has a certain impact on the dynamic response of the tail beam. However, the size of discrete element particles is in millimeters, and the shape of the particles cannot represent the macro shape of coal gangue after crushing. Therefore, in the process of multi-domain collaborative simulation, the shape of discrete element particles should be set to circular (A = 1.0).

5.4 Feasibility verification

Based on interface technology, the characteristic information obtained by EDEM–RecurDyn–AMESim multi-field caving support–scraper conveyor machine-fluid integrated collaborative simulation is consistent with the characteristic information of the actual caving process measured in the coal mine, which determines the theoretical significance and engineering application value of the research on fully mechanized caving based on this method.

Industrial tests were carried out on 1109 fully mechanized top-coal caving face in Baiyinhua No. 4 mine. The vibration acceleration of the tail beam measured using the vibration sensor (Zhu, 2014; Xue et al., 2015) installed in the belly of the tail beam is shown in Figure 19.

Analysis of the data plot measured downhole in Figure 19 shows that the amplitude is between 2g and 3g, and the waveform has symmetry. The results of the simulation analysis show that the amplitude is between 2g and 3g when the particle radius is 20 mm, the waveform is symmetrical when the standard deviation is 0.05 and slenderness ratio A = 1.0, and the vibration acceleration of the tail beam is obtained by simulation parameters with particle radius 20 mm, standard deviation 0.05, and slenderness ratio A = 1.0, as shown in

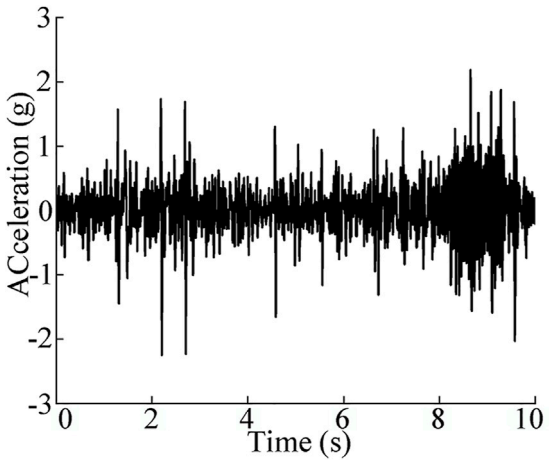

FIGURE 19
Downhole measured data.

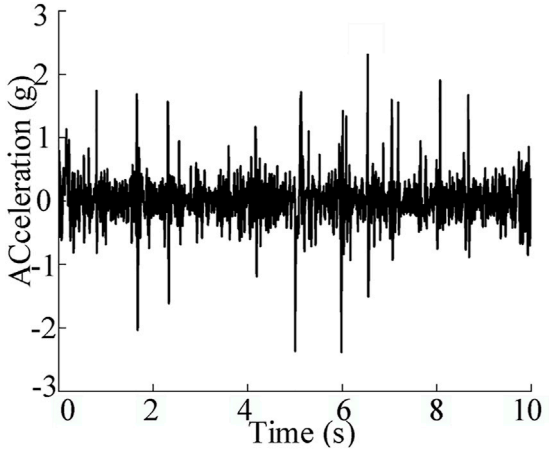

FIGURE 20
Data from simulation.

Figure 20. The vibration characteristic values are shown in Table 6. From the 19 diagrams, Figure 20, and Table 6, it can be seen that the relative error of the maximum, minimum, and root mean square values of the tail beam vibration is only 3.8%, 5.5%, and 14%, respectively, which are within a reasonable range.

In conclusion, the simulation results of virtual prototype simulation can be reliable by setting the particle radius as 20 mm, particle size distribution as normal distribution (standard deviation is 0.05), and slenderness ratio A = 1.0 when fully mechanized top-coal caving is simulated based on the EDEM–RecurDyn–AMESim multi-domain collaborative simulation method.

TABLE 6 Time-domain signal characteristics of tail beam vibration acceleration.

Tail beam vibration comparison (mm/s^2)	Maximum (mm/s^2)	Minimum (mm/s^2)	Root mean square value (mm/s^2)
Simulation value	23,832.3	−24641.5	3715.1
Test value	22,964.1	−23356.3	4343.4
Relative error	0.038	0.055	0.14

6 Conclusion

Aiming at the characteristics of discrete element particles which influence the simulation results of the top-coal caving process, this study puts forward a method of EDEM–RecurDyn–AMESim multi-field caving support–scraper conveyor hydraulic integrated co-simulation based on interface technology, and a research scheme on the influence of different particle sizes, distributions, and shapes on the dynamic response of tail beam is designed. Through time-domain and time–frequency domain analysis and research, the following conclusions can be drawn:

(1) The vibration of the tail beam is greatly affected by the choice of particle radius. The amplitude of vibration increases first and then decreases with the increase in particle radius. The main energy distribution frequency of the signal increases first and then decreases with the increase in particle radius. The amplitude of vibration increases first and then decreases with the increase in standard deviation. The frequency of energy distribution of the main frequency of signal increases gradually with the increase in standard deviation. When the standard deviation is not 0, the vibration signal is more symmetrical. The fluctuation time of the vibration signal gradually decreases with the increase in the slenderness ratio, and the amplitude first increases and then decreases with the increase in the slenderness ratio. The vibration signal is most symmetrical when the slenderness ratio is A = N/A. The frequency of main frequency energy distribution decreases with the increase in the slenderness ratio. The distribution of main frequency energy at A = N/A is similar to that at A = 1.

(2) Based on the virtual prototype technology, a virtual prototype simulation method of multi-field cooperation for fully mechanized top-coal caving is established, which solves the problems of difficult sampling in underground field, high risk coefficient, and high test cost. Combined with the vibration data of the tail beam measured in actual downhole, the particle setting parameters of the multi-domain collaborative simulation virtual prototype model for simulating the top-coal caving process are determined, which lays a foundation for subsequent research.

(3) This method can be widely used in the research and development of super-large caving support and scraper conveyor, reliability analysis of mining equipment, and recognition of fully mechanized caving gangue. It has the advantages of low cost, fast cycle, and high safety and provides reference for the research of intellectualization and unattended coal mines.

Data availability statement

The original contributions presented in the study are included in the article/Supplementary Material; further inquiries can be directed to the corresponding author.

Author contributions

LZ provided the materials, laboratory tools, and facilities. LZ planned and supervised the study. LH assisted with the model analysis and results. HZ and XJ carried out the simulation model construction, implementation of the experiment, experimental data analysis, image graphics, and manuscript writing and preparation. MG and SY assisted with the literature survey. All authors read and commented on the manuscript.

Funding

This work was supported by the National Natural Science Foundation of China [Grant number 51674134], the Liaoning Provincial Natural Science Foundation of China [Grant number 20170540420], and the Key projects of Liaoning Provincial Department of Education [Grant number LJ2017ZL001].

Conflict of interest

Author MG is employed by Shandong Yankuang Intelligent Manufacturing Co., Ltd.

The remaining authors declare that the research was conducted in the absence of any commercial or financial relationships that could be construed as a potential conflict of interest.

Publisher's note

References

Bharadwaj, R., Ketterhagen, W. R., and Hancock, B. C. (2010). Discrete element simulation study of a Freeman powder rheometer. *Chem. Eng. Sci.* 65 (21), 5747–5756. doi:10.1016/j.ces.2010.04.002

Bian, X. C., Li, W., Li, G. Y., and Erol, T. (2015). Three-dimensional discrete element analysis of railway ballast's shear process based on particles' real geometry. *J. Eng. Mech.* 32 (05), 64–75+83. doi:10.6052/j.issn.1000-4750.2013.11.1029

Cai, P. R., Chen, W., Lin, L. F., Chen, S. H., Shen, J. J., Yang, J., et al. (2020). Noise analysis of coastal broadband tiltmeter based on STFT method. *J.China Earthq. Eng. J.* 42 (02), 396–402. doi:10.3969/j.issn.1000-0844.2020.02.369

Chen, L., Wu, S. C., and Jin, A. B. (2021). Particle discrete element layered modeling method and particle size effect. *J. Southwest Jiaot. Univ.* doi:10.3969/j.issn.0258-2724.20210023

Cui, W., Wei, J., Wang, C., Wang, X. H., and Zhang, S. R. (2021). Discrete element simulation of collapse characteristics of particle column considering gradation and shape. *J. Chin. J. Geotechnical Eng.* 43 (12), 2230–2239. doi:10.11779/CJGE202112009

Han, Z. H., Zhang, L. Q., Zhou, J., and Wang, S. (2021). Effect of clay mineral grain characteristics on mechanical behaviours of hydrate-bearing sediments. *J. J. Eng. Geol.* 29, 1733–1743. doi:10.13544/j.cnki.jeg.2021-0052

Hu, B., and Chen, C. J. (2019). Analysis of influence of material characteristics on the structure of blanking pipe based on EDEM simulation technology. *J. Coal Qual. Technol.* 34 (05), 56–60.

Liu, C., Li, H. M., and Zhang, Q. L. (2018). Research on reasonable ratio of setting load and yield load of shield in large mining height coal mine. *J. J. Min. Saf. Eng.* 35 (04), 725–733. doi:10.13545/j.cnki.jmse.2018.04.009

Liu, R., Li, Y. J., Liu, Z. J., Liu, L. J., and Lv, H. T. (2021). How and when factors of agricultural contribution influence urbanization: A historical analysis of tibet. *Discrete Dyn. Nat. Soc.* 52, 1–15. doi:10.1155/2021/7255274

Luo, J. Y., Huang, G., Xiong, Y, T., and Zhang, L. (2016). Experimental study on the relationship between the distribution of micro coal particles and the crushing energy. *J. J. China Coal Soc.* 41 (12), 3054–3061. doi:10.13225/j.cnki.jccs.2016.0334

Mao, J., Liu, S. Y., Zhang, K., Liu, X. Y., and Wang, J. (2019). Simulation study on caving process of caving coal hydraulic supports based on edem. *J. J. Mech. Strength.* 41 (02), 468–472. doi:10.16579/j.issn.1001.9669.2019.02.035

Wang, J. C., Pan, W. D., Zhang, G. Y., Yang, S. L., Yang, K. H., and Li, L. H. (2022). Principles and applications of image-based recognition of withdrawn coal and intelligent control of drawing opening in longwall top coal caving face. *J. J. China Coal Soc.* 47 (01), 87–101. doi:10.13225/j.cnki.jccs.YG21.1530

Wang, J. C., Wei, L. K., Zhang, J. W., and Li, Z. L. (2013). 3-D numerical simulation on the top-coal movement law under caving mining technique. *J. J. China Coal Soc.* 38 (11), 1905–1911. doi:10.13225/j.cnki.jccs.2013.11.013

Wang, X. W., Qin, Y., Tian, Y. K., Yang, X. Y., and Yang, Z. J. (2015). Analysis on flow features of bulk coal during coal unloading period based on EDEM. *J. Coal Sci. Technol.* 43 (5), 130–134. doi:10.13199/j.cnki.cst.2015.05.032

Wang, X. W., Xu, G. Y., Zhu, G. H., and Ma, H. J. (2019). Research and analysis on gate angle of feeding system based on EDEM. *J. .Coal Eng.* 51 (07), 142–145. doi:10.11799/ce201907031

Wang, Y. D., Zhao, L. J., and Zhang, M. C. (2021). Research on self-adaptive height adjustment control strategy of shearer. J/OL. *J. China Coal Soc.* doi:10.13225/j.cnki.jccs.2021.1371

Wu, X. W. (2010). *The Mechanical-hydraulic co-simulation of the hydraulic support and the analysis of hydraulic control system*. Qing dao: Shandong University of science and technology.

Xi, Y. (2020). Analysis on the influence factor of seismic deconvolution based on sampling theorem. *J. Contemp. Chem. Ind.* 49 (04), 724–727. doi:10.13840/j.cnki.cn21-1457/tq.2020.04.053

Xinliang, Tian., Xu, Chong., Jiangtao, Qi., Hui, Guo., Mao, Li., and Xuhui, Mao. (2021). Parameter calibration of discrete element model for corn straw - soil mixture in black soil areas. *J .Transactions Chin. Soc. Agric. Mach.* 52 (10), 100–108+242. doi:10.6041/j.issn.1000-1298.2021.10.010

Xue, G. H., Zhao, X. Y., Liu, E. M., Hu, B. H., and Ding, W. J. (2015). Time-domain characteristic extraction of coal and rock vibration signal in fully-mechanized top coal caving face. *J. Coal Sci. Technol.* 43 (12), 92–97. doi:10.13199/j.cnki.cst.2015.12.019

Yang, Y., and Zeng, Q. L. (2021). Impact-slip experiments and systematic study of coal gangue "category" recognition technology Part I: Impact-slip experiments between coal gangue mixture and top coal caving hydraulic support and the study of coal gangue "category" recognition technology. *Powder Technol.* 392, 224–240. doi:10.1016/j.powtec.2021.06.055

Yang, Y., and Zeng, Q. L. (2022). Impact-slip experiments and systematic study of coal gangue "category" recognition technology part II: Improving effect of the proposed parallel voting system method on coal gangue "category" recognition accuracy based on impact-slip experiments. *Powder Technol.* 395, 893–904. doi:10.1016/j.powtec.2021.08.097

Yu, X. Y., Wang, Z. S., Yang, Y., and Mao, X. W. (2021). Numerical study on the movement rule of overburden in fully mechanized caving mining with thick depth and high mining height. *J. J. Min. Strata Control Eng.* 3 (1), 28–38. doi:10.13532/j.jmsce.cn10-1638/td.20200715.001

Zhang, C. G., Yin, Z. Y., Wu, Z. X., and Jin, Y. F. (2019). Three-dimensional discrete element simulation of influence of particle shape on granular column collapse. *J .Rock Soil Mech.* 40 (03), 1197–1203. doi:10.16285/j.rsm.2017.2065

Zhang, M. C., Zhao, L. J., and Wang, Y. D. (2021). Recognition system of coal-rock cutting state based on CPS perception analysis. *J. J. China Coal Soc.* 46 (12), 4071–4087. doi:10.13225/j.cnki.jccs.2021.0236

Zhang, W. S., Zhang, R. Y., Chen, T. Y., Fu, J., and Yuan, H. F. (2022). Calibration of simulation parameters of mung-been seeds using discrete element method and verification of seed-u03), 71–79.

Zhang, X., Qiao, W., Lei, L. J., Zeng, F. S., Zhang, H., and Wang, Y. Z. (2016). Formation mechanism of overburden bed separation in fully mechanized top-coal caving. *J. J. China Coal Soc.* 41, 342–349. doi:10.13225/j.cnki.jccs.2015.1992

Zhao, L. J., Jin, X., Zhao, Y. D., and Wang, B. (2020). Discrete element simulation analysis on the wear characteristics of drum in coal seam with gangue. *J. J. China Coal Soc.* 45 (9), 3341–3350. doi:10.13225/j.cnki.jccs.2019.0843

Zhao, L. J., Wen, S. J., and Liu, X. N. (2020). The influence of simulated particle radius on complex coal seam of drum cutting. *J. Mech. Sci. Technol. Aerosp. Eng.* 39 (01), 52–57. doi:10.13433/j.cnki.1003-8728.20190090

Zhu, S. G. (2014). *Study on coal and rock character recognition method in fully mechanized caving faces*. Bei jing), Bei jing: China University of mining and technology.